Hindawi
Science and Technology of Nuclear Installations
Volume 2018, Article ID 5327146, 17 pages
https://doi.org/10.1155/2018/5327146

Research Article

Assessment of Neutronic Characteristics of Accident-Tolerant Fuel and Claddings for CANDU Reactors

Simon Younan and David Novog

McMaster University, Hamilton, ON, Canada

Correspondence should be addressed to David Novog; novog@mcmaster.ca

Received 29 August 2017; Revised 28 November 2017; Accepted 10 December 2017; Published 1 March 2018

Academic Editor: Tomasz Kozlowski

The objective of this study was to evaluate accident-tolerant fuel (ATF) concepts being considered for CANDU reactors. Several concepts, including uranium dioxide/silicon carbide (UO_2-SiC) composite fuel, dense fuels, microencapsulated fuels, and ATF cladding, were modelled in Serpent 2 to obtain reactor physics parameters, including important feedback parameters such as coolant void reactivity and fuel temperature coefficient. In addition, fuel heat transfer was modelled, and a simple accident model was tested on several ATF cases to compare with UO_2. Overall, several concepts would require enrichment of uranium to avoid significant burnup penalties, particularly uranium-molybdenum (U-Mo) and fully ceramic microencapsulated (FCM) fuels. In addition, none of the fuel types have a significant advantage over UO_2 in terms of overall accident response or coping time, though U-9Mo fuel melts significantly sooner due to its low melting point. Instead, the different ATF concepts appear to have more modest advantages, such as reduced fission product release upon cladding failure, or reduced hydrogen generation, though a proper risk assessment would be required to determine the magnitude of these advantages to weigh against economic disadvantages. The use of uranium nitride (UN) enriched in ^{15}N would increase exit burnup for natural uranium, providing a possible economic advantage depending on fuel manufacturing costs.

1. Introduction

While there are many studies evaluating the performance of accident-tolerant fuels (ATF) in light water reactors (LWRs), there are comparatively few studies which look at the use of ATF in CANDU reactors. ATF has the potential to reduce the consequences of a severe accident and/or give the operators more time to mitigate the consequences of a severe accident. However, as there are significant differences between LWRs and CANDU reactors in terms of reactor and fuel design, ATF should be evaluated specifically for CANDU reactors in order to determine their viability for future use in CANDU reactors.

This study in particular focused primarily on reactor physics, using Serpent 2 to evaluate the CANDU fuel lattice behaviour for different ATF loadings. While thermal hydraulics were not specifically modelled for this study, heat transfer from the fuel is a key consideration for accident-tolerant fuel and has a significant effect on the reactor physics; thus simple heat transfer models were constructed in order to calculate fuel temperatures for each case. The accident-tolerant fuel cases include the following:

(i) Uranium dioxide/silicon carbide (UO_2-SiC) composite fuel

(ii) High-density fuels: uranium nitride (UN), uranium silicide (U_3Si_2) (as an additive to UN), and uranium-molybdenum alloy fuel (U-9Mo)

(iii) Fully ceramic microencapsulated (FCM) fuels

(iv) Accident-tolerant cladding materials.

2. Literature Review

Most power reactors rely on fuel consisting of uranium dioxide pellets surrounded by a zircaloy sheath. UO_2 is preferred over uranium metal due to greater stability and a high melting point (roughly 2850°C) but has a disadvantage of a poor

thermal conductivity, particularly at higher temperatures and irradiation levels [1]. This leads to large temperature gradients and thermal stresses. The fuel pellets retain most of the fission products, while the cladding acts as a second barrier [2] to contain fission products that escape from the pellets. Zirconium alloys are preferred for the cladding due to a low thermal neutron capture cross-section. However, under degraded-cooling conditions, cladding temperatures can become high enough to initiate a zirconium-steam oxidation reaction which may produce significant amounts of hydrogen gas.

Accident progression in CANDU reactors differs from that in LWRs. In the case of a loss-of-coolant accident (LOCA) or station blackout (SBO) where cooling is degraded, heat removal may still occur via radiation to the pressure tube. As the pressure tube heats up, it will balloon or sag, depending on system pressure, until it touches the calandria tube, in which case heat can be conducted to the moderator. The large volume of water in the moderator can then sustain a heat sink for a prolonged period, providing operators with a significant window to implement emergency procedures [3]. A significant radionuclide release to containment would only occur if moderator cooling is unavailable and the moderator is lost as a heat sink.

Studies of accident-tolerant fuels have increased since the Fukushima disaster, where a SBO scenario led to fuel cladding oxidation, fuel melting, hydrogen explosions, and the release of radiation into the environment [4]. Accident-tolerant fuel can be used to reduce the potential consequences of an accident by limiting the release of fission products, reducing fuel and sheath temperatures, limiting hydrogen production, improving heat transfer, and/or mitigating the event entirely [5].

The simplest proposal for accident-tolerant fuel is to mix up to 10% silicon carbide by volume into UO_2, forming composite pellets through spark plasma sintering [6]. The high thermal conductivity of silicon carbide improves the thermal conductivity of the mixture significantly, without significantly impacting neutron economy. A 10% SiC addition can improve thermal conductivity by 62% and reduce centre-line temperatures by 20% [6], improving fission product retention within fuel pellets. Studies have also shown that diamond could also be used in a similar manner [7]. Beryllium oxide could also be mixed with UO_2 [8], though its use is complicated by the toxicity of beryllium.

Uranium nitride has been proposed as an accident-tolerant fuel due to a much greater thermal conductivity and greater uranium density compared to UO_2, while still having a high melting point. Typical impurity levels can be kept well below 1% [9], and, at reactor operating temperatures, the thermal conductivity of UN can exceed that of UO_2 by a factor of 5 or more [1, 10]. However, ^{14}N has very poor neutron economy, so in CANDU it requires either significant enrichment of the uranium to compensate, or enrichment of the nitrogen to ^{15}N. Also, uranium nitride can react with water [11], which is potentially an issue for accidents where sheath integrity is lost.

Uranium silicide (U_3Si_2) has been proposed as a compromise between UO_2 and UN, with uranium density and thermal conductivity between the two, along with a neutron economy similar to UO_2 and less reactivity with water compared to UN, though with a lower melting point than either. Uranium silicide can also be mixed into uranium nitride to combine their properties. The uranium silicide would protect the uranium nitride from exposure, while still providing a better thermal conductivity than UO_2 [11]. The compound U_3Si_2 is used as it provides a higher uranium density than USi_2 and USi, while U_3Si dissociates at 900°C, making U_3Si_2 the ideal choice for power reactor applications [12].

Another proposal is for uranium-molybdenum alloys, with a high uranium density, good thermal conductivity, and a fair neutron economy, though with a rather low melting temperature. With a melting point of only around 1400 K [13], this presents potential issues for use in CANDU, as the progression of some accidents predict temperatures well in excess of this melting point [14]. Uranium metal possesses both an α-phase and a γ-phase. The γ-phase has superior properties but can only exist well above room temperature. The addition of molybdenum makes the γ-phase metastable at room temperature [13]. Even then, the material can still corrode if exposed to water, so an additional corrosion barrier such as aluminum, chromium, or niobium can be diffused into the metallic pellets [15]. Overall, the thermal conductivity is much greater than that of UO_2 and even greater than UN at elevated temperatures [16].

One final option for the fuel pellets is to manufacture fully ceramic microencapsulated (FCM) fuel. In this fuel, uranium dioxide or uranium nitride is embedded within tristructural-isotropic (TRISO) particles, which use several layers, including a silicon carbide layer, to contain fission products [10]. In addition, the TRISO particles are embedded within a silicon carbide matrix, acting as an additional fission product barrier. The high thermal conductivity of silicon carbide results in low fuel temperatures. However, since much of the fuel volume is inert, higher enrichments are generally required to compensate. One compromise is to embed bare spheres of fuel within the matrix, rather than TRISO particles, allowing for more fissile material to be packed into the fuel elements, while still providing low temperatures and better fission product retention than UO_2. Fuel kernels can be UO_2 or UN, with UN generally preferred for its greater uranium density. In the case of using FCM fuel in LWRs, an enrichment of up to 19.9% may be needed to maintain current cycle lengths [10, 15]. One option which may be permitted by the improved thermal conductivity is a change in the assembly pitch, where the 16 × 16 assembly is replaced by a 12 × 12 assembly with larger pins, allowing for an increased fuel volume and reducing the enrichment to roughly 15% [10]. Changing the particles to bistructural-isotropic (BISO) particles [15], or even bare kernels in a SiC matrix, could allow for more uranium to be packed into the fuel and reduce the required enrichment.

The thermal conductivity of SiC is particularly susceptible to irradiation-induced degradation [15]. As a result, fuel temperatures could increase significantly as SiC-containing fuel is irradiated. However, the thermal conductivity will still be significantly better than that of UO_2, especially at elevated temperatures where the thermal conductivity saturates at a higher value [17].

In terms of cladding, modifications fall under three categories: metallic cladding, ceramic cladding (SiC), and multilayer claddings or surface coatings. Replacing the zircaloy cladding with another alloy such as stainless steel or iron-chromium-aluminum alloy (FeCrAl) [18] can improve oxidation resistance during an accident. However, steels tend to weaken and melt at lower temperatures compared to zirconium-based alloys [15], so molybdenum-based alloys have also been proposed as an alternative that can withstand high temperatures [19]. However, these metals capture more neutrons compared to zirconium and thus reduce the fuel's neutron economy significantly. It would not be practical to use these claddings as a full layer due to the impact on neutron economy, especially in the CANDU system which depends on a high neutron economy. However, as steels are generally stronger than zirconium alloys, the cladding could potentially be made thinner [20], potentially making up for the neutron economy penalty by increasing the volume of uranium.

The zircaloy cladding can also be replaced by a SiC-based cladding. Unlike metals, SiC is virtually transparent to neutrons and also has a significantly higher melting point than stainless steels. However, silicon carbide is relatively brittle compared to metals, increasing the risk of failure due to thermal and mechanical stresses. Some proposals have been made to mitigate this issue, such as producing SiC fibres rather than monolithic SiC and embedding the fibres to form a composite, though this has the disadvantage of being permeable to fission products [21]; thus a combination of monolithic and composite SiC would be needed for fission product retention. Overall, the implementation of SiC cladding is complicated by a lack of familiarity in its potential use as nuclear fuel cladding, compared with metallic cladding which would behave mechanically similarly to zircaloy [20, 22].

The final option is simply coating the zircaloy with an oxidation-resistant material, either metallic or ceramic. This provides the oxidation resistance of the surface material while retaining the mechanical properties of the zircaloy and greatly reducing the impact on neutron economy as less neutron-absorbing material is used. The burnup penalty is minimal when compared to monolithic FeCrAl [22]. Some disadvantages in this approach include stresses from differential thermal expansion and possible diffusion between the two metal layers to create an intermetallic layer [20], which the monolithic layer would avoid. This study includes a case where a FeCrAl surface layer is added over zircaloy to protect it without a large penalty to neutron economy. For a pressurized water reactor (PWR), if the FeCrAl clad thickness can be reduced to 300 μm, an increase in enrichment can be avoided without impacting the cycle length, due to increased uranium loading from the use of larger fuel pellets [23]. Meanwhile, SiC cladding has a better neutron economy than zircaloy, but if the cladding must be made significantly thicker, the reduced fuel volume may lead to higher enrichment requirements [23]. Overall, the use of steel cladding is expected to increase fuel costs [23].

The following properties for accident-tolerant fuel materials have been identified in Tables 1 and 2 and in Figure 1.

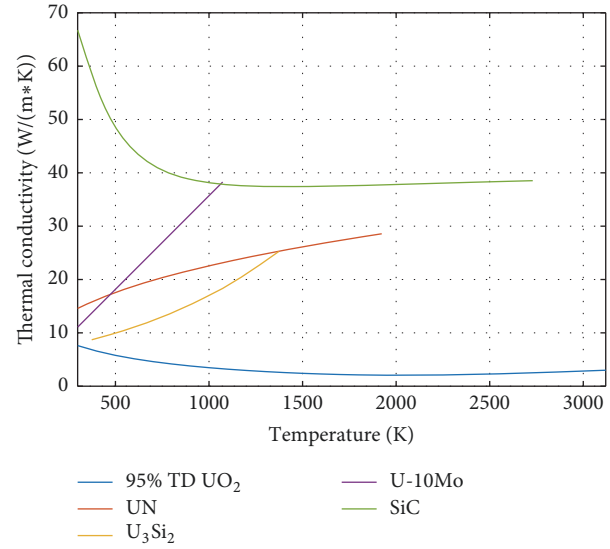

Figure 1: Comparison of thermal conductivity of UO_2 and ATF materials [1, 10, 11, 16].

Table 1: Uranium density comparison for UO_2 and ATF fuel.

Fuel material	Uranium density (g/cm^3)	Ref.
UO_2 (fully dense)	9.66	[11]
UO_2 (5% porosity)	9.18	
UN (fully dense)	13.55	[11]
U_3Si_2 (fully dense)	11.31	[11]
U-8Mo (fully dense)	16.1	[13]
FCM UO_2/SiC (55% TRISO packing)	1.84	[10]
FCM UN/SiC (55% TRISO packing)	2.72	[10]

Table 2: Melting points for UO_2 and ATF fuel materials.

Fuel material	Melting point (°C)	Ref.
UO_2	2847	[24]
UN	2680	[25]
U_3Si_2	1665	[24, 25]
U-8Mo	1135	[13]
SiC	2457	[10]

3. Methodology

The fuels evaluated in this study were as follows:

(i) UO_2/SiC composite fuel

(ii) Uranium nitride fuel (enriched to 99.5% ^{15}N)

(iii) UN/U_3Si_2 composite fuel

(iv) UN fuel mixed with zirconium nitride (as (U, Zr)N solution)

(v) U-9Mo fuel

(vi) FCM with UO_2 and UN in SiC, assuming bare kernels embedded in the matrix to maximize fuel loading, thus acting more like a microcell fuel

Table 3: ATF case table analyzed.

Case	Fuel	Cladding	Target BU (MWh/kgU)
(0)	Uranium dioxide	Zircaloy-4	200 (NU)
(1)	Uranium dioxide	Zircaloy-4	600
(2)	UO_2 + 3% SiC by volume	Zircaloy-4	NU, 200, 600
(3)	UO_2 + 3% SiC by volume	SiC	200
(4)	UO_2 + 3% SiC by volume	Zr/FeCrAl	200
(5)	UO_2 + 6% SiC by volume	Zircaloy-4	200
(6)	UO_2 + 10% SiC by volume	Zircaloy-4	200
(7)	Uranium nitride	Zircaloy-4	NU, 600
(8)	UN + 3% U_3Si_2 by volume	Zircaloy-4	NU
(9)	UN + 6% U_3Si_2 by volume	Zircaloy-4	NU
(10)	UN + 10% U_3Si_2 by volume	Zircaloy-4	NU
(11)	UN + 10% ZrN by volume	Zircaloy-4	NU
(12)	U-9Mo	Zircaloy-4	200
(13)	FCM, UO_2 kernels in SiC, 40% packing, 700 μm diameter	Zircaloy-4	NU, 200, 600, ∗
(14)	FCM, UO_2 kernels in SiC, 45% packing, 700 μm diameter	Zircaloy-4	200, ∗
(15)	FCM, UO_2 kernels in SiC, 35% packing, 700 μm diameter	Zircaloy-4	200, ∗
(16)	FCM, UO_2 kernels in SiC, 40% packing, 650 μm diameter	Zircaloy-4	200, ∗
(17)	FCM, UO_2 kernels in SiC, 40% packing, 750 μm diameter	Zircaloy-4	200, ∗
(18)	FCM, UO_2 kernels in SiC, 50% packing, 700 μm diameter	Zircaloy-4	200, ∗
(19)	FCM, UO_2 kernels in SiC, 55% packing, 700 μm diameter	Zircaloy-4	200, ∗
(20)	FCM, UN kernels in SiC, 40% packing, 700 μm diameter	Zircaloy-4	200, ∗
(21)	FCM, UN kernels in SiC, 45% packing, 700 μm diameter	Zircaloy-4	200, ∗
(22)	FCM, UN kernels in SiC, 35% packing, 700 μm diameter	Zircaloy-4	200, ∗
(23)	FCM, UN kernels in SiC, 50% packing, 700 μm diameter	Zircaloy-4	200, ∗
(24)	FCM, UN kernels in SiC, 55% packing, 700 μm diameter	Zircaloy-4	200, ∗
(25)	FCM, UN TRISO in SiC, 55% packing, 700 μm diam. kernels	Zircaloy-4	∗

∗ indicates exit burnup of 4044 MWh/bundle.

(vii) FCM with UN TRISO particles in SiC

(viii) Silicon carbide cladding

(ix) Two-layer cladding using zircaloy with a 20% thickness FeCrAl layer. The cladding consists of a zircaloy layer of 80% of the nominal CANDU cladding thickness, with the FeCrAl coating thickness of 20% of the nominal CANDU cladding thickness, so that the total thickness is the same as for the standard zircaloy cladding.

The full case list is shown in Table 3.

Several different exit burnups were evaluated. Nearly all cases were evaluated for an exit burnup of 200 MWh/kgU. As the calculations were for a lattice and not a full core, an average excess reactivity was calculated for natural UO_2 and the exit burnup for all other cases calculated based on this excess reactivity. Some cases were also computed at a higher exit burnup of 600 MWh/kgU. However, for an exit burnup of 200 MWh/kgU, the average residence time of the fuel is proportional to the fuel's uranium density. This is of particular concern for FCM fuel, which has a very low uranium density. As 200 MWh/kgU is equivalent to 4044 MWh/bundle for UO_2 fuel as modelled in this study, cases for FCM fuel with an exit burnup of 4044 MWh/bundle were added.

For this study, the Serpent 2 code [26] was used to model an infinite 2D lattice of CANDU bundles in fuel channels, with fuel, channel, and lattice properties shown in Table 4. For FCM fuel, the model was extruded to one bundle length and the volume inside the fuel pins randomly filled with fuel particles, the methodology for which is built into Serpent 2. FlexPDE [27] was used to calculate fuel temperatures in one dimension, using the fission power distribution from Serpent along with temperature-dependent thermal conductivity values for each material. Fuel-clad contact resistance along with convection into the coolant was modelled as constant boundary conditions.

The research steps are shown in Figure 2.

3.1. Determination of Enrichment. To calculate the enrichment required for each case, the excess reactivity of each case is defined as follows:

$$\overline{\rho} = \frac{1}{B_{\text{exit}}} \int_0^{B_{\text{exit}}} \rho(B)\, dB. \quad (1)$$

Table 4: CANDU lattice properties.

Element	Property	Units	Value				Comment
Fuel	Temperature	K	941.29				
	Diameter	cm	1.2244				
Cladding	Temperature	K	560.66				
	OD*	cm	1.308				
Fuel bundle	Type		37-element				
	Number of pins		1	6	12	18	
	Ring radii	cm	0	1.5	2.9	4.35	
	Ring pitches	°	0	0	15	0	
Coolant	Composition		D_2O				
	Density	g/cm^3	0.81212				99.2% purity
	Temperature	K	560.66				
Pressure tube	Composition		Zr-Nb Alloy				
	Density	g/cm^3	6.57				97.5 wt% Zr 2.5 wt% Nb
	Temperature	K	560.66				
	ID**	cm	10.3378				
	OD	cm	11.2064				
Gas Gap	Composition		CO_2				
	Density	g/cm^3	0.002297				
	Temperature	K	345.66				
Calandria tube	Composition		Zr Alloy				
	Density	g/cm^3	6.44				97.24 wt% Zr 1.6 wt% Fe 1.1 wt% Cr 0.06 wt% Ni
	Temperature	K	345.66				
	ID	cm	12.8956				
	OD	cm	13.1750				
Moderator	Composition		D_2O				
	Density	g/cm^3	1.082885				99.91% purity
	Temperature	K	345.66				
Lattice pitch		cm	28.575				

*Outer diameter. **Inner diameter.

The integral was computed for each burnup case using the trapezoid method. An excess reactivity of roughly 35 mk was calculated for the base UO_2 case. Therefore, the enrichments of other cases were varied until they came within 1-2 mk of the same 35 mk excess reactivity, which accounts for leakage and reactivity devices.

The following equation was used to compute the concentration of ^{234}U with respect to enrichment [28]:

$$e_{234} = 0.0015 + 0.0058e_{235} + 0.000054e_{235}^2. \quad (2)$$

The ENDF/B-VII.0 libraries provided with Serpent were used, and Doppler Broadening Rejection Correction (DBRC) [29] was enabled for ^{238}U for energies from 0.4 eV to 210 eV. Enabling DBRC adjusts the scattering angle calculation to account for thermal motion of nuclei, which has the most significant impact near resonances. When DBRC is enabled for the depletion calculation and/or the fuel temperature coefficient (FTC) calculation, the k_{eff} results are affected to some extent, as shown in Figure 3.

Table 5: Serpent 2 burnup calculation parameters.

Parameter	Value
fpcut	10^{-9}
ttacut	10^{-18}

Enabling DBRC for depletion calculations has a noticeable effect on k_∞. Enabling DBRC for reactivity calculations has a substantial effect on k_∞, particularly at higher fuel temperatures. FTC predictions by Serpent using DBRC are therefore slightly more negative than predictions by other codes that do not implement DBRC or other corrections. The difference is on the order of 0.1 pcm/K in the temperature range of interest, which is significant enough to warrant the use of DBRC for neutron transport for CANDU.

For burnup calculations, the fuel was split into four depletion regions, with one for each ring of pins. The burnup parameters shown in Tables 5 and 6 were used.

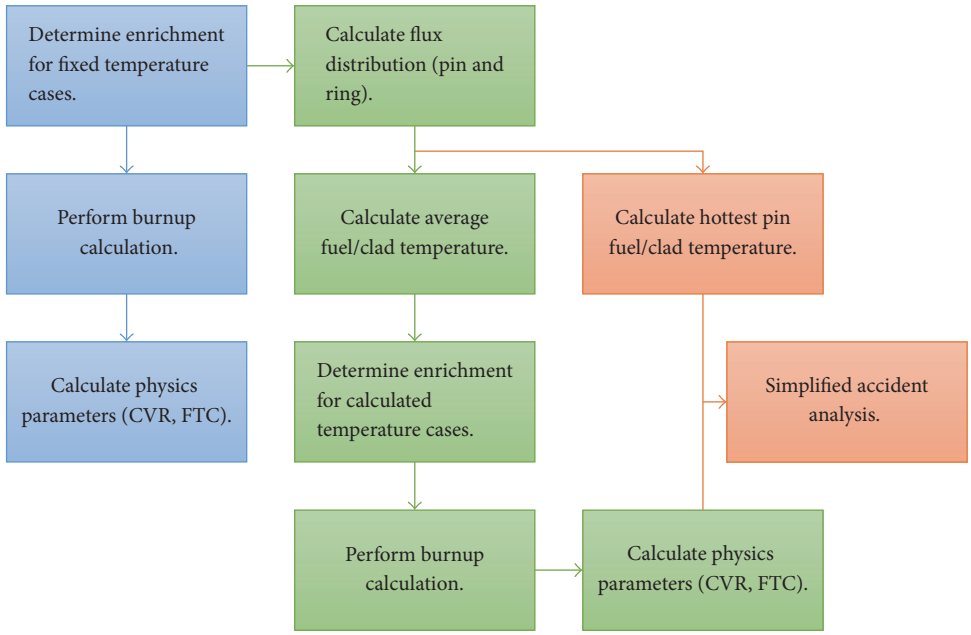

Figure 2: Methodology process.

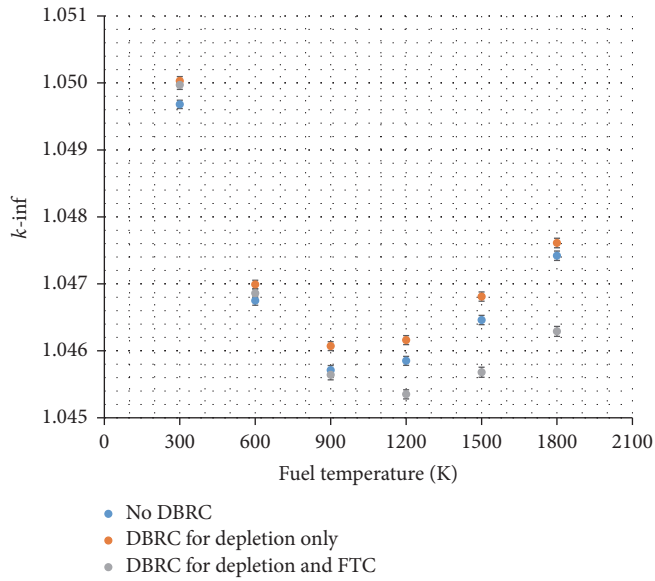

Figure 3: Effect of DBRC on CANDU lattice calculations.

The predictor-corrector method was enabled with linear interpolation and linear extrapolation to reduce the error in the computation of the irradiated nuclide densities. Unresolved resonance probability sampling was turned off (the default in Serpent) as its effect on thermal systems is relatively small. A bundle power of 700 kW was used for the burnup calculation. In all cases, the fuel temperature was assumed to be constant throughout the fuel cycle.

In addition, supplemental Serpent 2 runs were performed to obtain the exit burnup for each material as a function of enrichment. This allows the required enrichment for a specific burnup to be interpolated even for the cases which were not fully analyzed and allows for a better comparison of the different fuels in terms of enrichment.

3.2. Determination of Reactor Physics Parameters. For each case, the coolant void reactivity (CVR) and fuel temperature coefficient (FTC) were calculated for fresh fuel and for a burnup of 4 MWd/kg(U) or 96 MWh/kg(U). For the cases where the exit burnup exceeded 200 MWh/kg(U), an additional step closest to midburnup was selected from which to compute the CVR and FTC. For the CVR, the reactivity difference between the reference branch and coolant-voided branch was computed. The number of histories used was chosen to get

Table 6: Serpent burnup calculation steps.

Step	Burnup (MWd/kg(U))
0	0
1	0.03
2	0.06
...	...
7	0.21
8	0.25
9	0.30
10	0.45
11	0.60
...	...
15	1.20
16	1.50
17	1.80
18	2.10
19	2.50
20	3.00
21	3.50
...	...
26	6.00
27	7.00
28	8.00
29	9.00
30	10.00
...	...
50	30.00

sufficiently precise results. For the FTC, the fuel temperature was perturbed by 100 K in each direction. A greater number of neutron histories were used to improve the precision of the results.

3.3. Determination of Fuel Temperature. To calculate the flux distribution for the temperature calculation, each pin was binned into bins equally spaced by radius, with five bins for non-FCM fuel and 20 bins for FCM fuel.

For non-FCM fuel, the following equation is fit to the flux distribution given by Serpent 2 along with the total power of 700 kW for the bundle, with Q_0 and κ being variable:

$$Q(r) = Q_0 I_0(\kappa r). \tag{3}$$

The quantity κ is adjusted such that the weighted sum of square errors is minimized, while Q_0 is directly related to κ due to the total bundle power being fixed.

For FCM fuel, the power distribution is modelled directly as a piecewise function in FlexPDE. To determine the average pin temperature, the power for each bin is averaged amongst all 37 pins to get the power distribution. For the maximum pin temperature, the following multiplication is performed, where $\overline{Q_{\text{pin}}}$ is the average pin power for the entire bundle and $\overline{Q_{\text{outer}}}$ is the average pin power for the outermost ring of pins, which are the hottest:

$$Q_{\text{hot}}(r) = Q(r) * \frac{880\,\text{kW}}{700\,\text{kW}} * \frac{\overline{Q_{\text{outer}}}}{\overline{Q_{\text{pin}}}}. \tag{4}$$

Thermal conductivities and relations for mixtures were looked up in literature [30], ignoring the effects of irradiation on thermal conductivity due to incomplete data. A coolant temperature of 560.66 K was used, and the heat transfer coefficient was fixed at 45000 W/(m^{2}K). The contact conductance between fuel and cladding was fixed at 80000 W/(m^{2}K).

For the TRISO fuel, the properties shown in Table 7 were used.

3.4. Accident Transient Analysis. The final stage of the assessment involved modelling a simplified large break LOCA with loss of ECC. This can be considered to be the most serious credible loss of heat sink accident for CANDU, as the heat sink is lost almost immediately and the net-energy deposited in the first few seconds is significant. The model employed here is simplified as the thermal hydraulic circuit was not explicitly modelled in this study, but instead the thermal hydraulic data was modelled using information and data on large break LOCAs obtained from literature [31–33], and thus the thermal hydraulic behaviour was the same for all cases. The goal, rather, was to look at the effect on neutronics, using CVR and FTC as reactivity feedback in a point kinetics model, from which other neutronic parameters were calculated in Serpent 2, along with looking at the effect on the temperature of the fuel, to determine the relative potential for fuel damage.

In summary, the thermal hydraulics involved a blowdown period where some cooling is sustained. After the initial power transient, the reactor would trip so that fission power would drop to near zero; thus the fuel would initially cool under these blowdown conditions. After the blowdown period the coolant would stagnate and the convection of heat to the coolant would drop to nearly zero, so the fuel would heat up due to decay heat. Radiation of heat between the rings of pins and the pressure tube was modelled during this phase, with the pressure tube deformation to the calandria assumed to occur at 1200 K.

The reactivity feedback due to coolant voiding, based on a two-loop, two-pass CANDU design, was

$$\rho_{\text{cv}}(t) = \text{CVR}\left(0.25\alpha_1(t) + 0.25\alpha_2(t) + 0.5\alpha_3(t)\right). \tag{5}$$

The core reactivity with all feedback was modelled by

$$\rho(t) = \text{FTC}\left(\overline{T}(t) - \overline{T}_{ss}\right) + \rho_{\text{cv}}(t) + \rho_{\text{SDS1}}(t). \tag{6}$$

For each case, the transient was modelled in two steps. The first step only included the "average" pin and modelled the point kinetics with one delayed group. The second step modelled the pins of the four rings along with the pressure tube, using the fission power history calculated in the first step.

The progression of the loss of coolant in the model is given in Figure 4.

Table 7: Composition of TRISO particle [10].

Layer	Material	Outer radius (μm)	Vol. Frac. (%)	Thermal conductivity (W m^{-1} K^{-1})
Kernel	UN	350	36.4	Temperature dependent
Buffer	Low-density PyC	400	18.0	0.5
Inner PyC	High-density PyC	435	15.6	4
SiC Coating	SiC	470	18.3	Temperature dependent
Outer PyC	High-density PyC	490	11.8	4

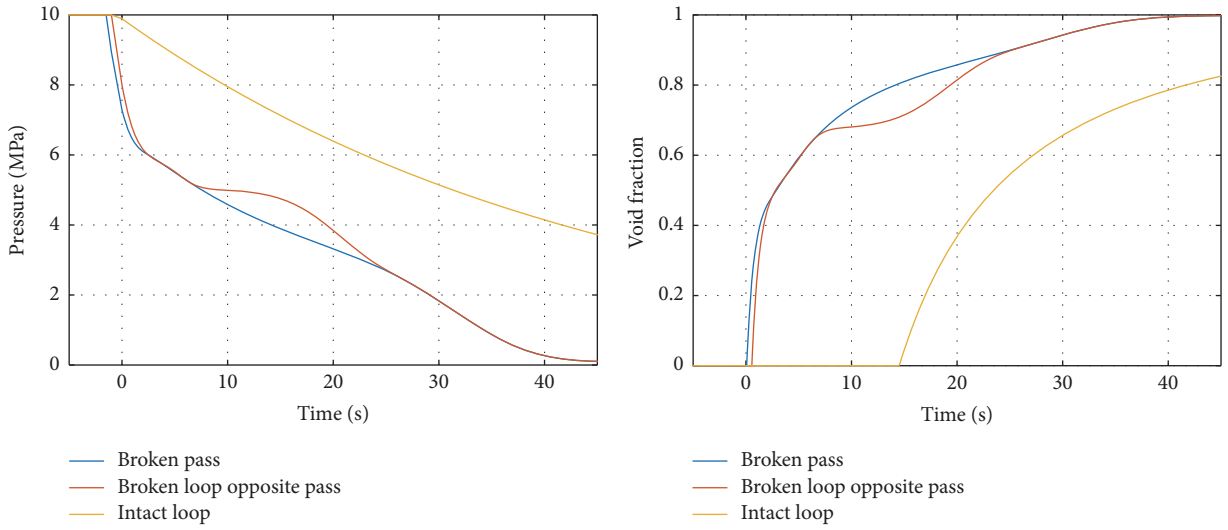

Figure 4: HTS pressure and void fraction behaviour for stylized transient.

4. Results

4.1. Determination of Enrichment. Certain ATF selections required a greater enrichment than other cases. As silicon carbide captures very few neutrons; the UO_2-SiC composite fuels only require minimal enrichment to provide the same exit burnup. U-9Mo requires slight enrichment (0.93%) due to the neutrons captured by molybdenum isotopes. For uranium nitride, if natural nitrogen were used, a significant enrichment of the uranium would be required. However, by enriching the nitrogen instead, natural uranium can be used and the exit burnup exceeds the 200 MWh/kg(U) for UO_2 bundles. As the uranium density is greater for the UN bundles, the 4044 MWh/bundle of UO_2 bundles is exceeded by UN bundles by enriching only the nitrogen. For FCM fuel, the enrichment requirements are increased due to the replacement of fissile material with inert material. However, this effect becomes stronger when the exit burnup is increased to compensate for the low uranium density of the fuel. Reducing the packing fraction increases enrichment requirements further due to reduction of the uranium density. As UN kernels contain more uranium than UO_2 kernels, the enrichment requirements are less for UN kernels than UO_2 kernels. The TRISO fuel has the lowest uranium mass and therefore requires the highest enrichment to achieve a similar bundle lifetime.

Table 8 and Figure 5 lists the required enrichments to achieve certain exit burnup targets. In the uranium nitride cases, the exit burnup for natural uranium exceeds that of natural UO_2, so the exit burnup values calculated for each case are listed. The relationship between enrichment and packing fraction for FCM-type fuel is listed in Figure 6.

4.2. Determination of Fuel Temperature. In all cases, the fuel temperatures calculated for the ATF fuel pins are less than those for the UO_2 fuel pins, as shown in Figure 7 and Table 10. The most modest results are obtained for the UO_2-SiC composite cases. However, even with only 10% SiC added, the maximum centre-line temperature decreases from 2070 K to 1464 K, or by roughly 30%. When irradiation is accounted for in the thermal conductivity calculations, a midburnup bundle has a maximum centre-line temperature of 2306 K for UO_2 and 1881 K for UO_2-10% SiC, which is approximately a 20% temperature reduction, as shown in Table 9. For all the other ATF pellet materials, the maximum centre-line temperature is below 1000 K, and it is around 800 K for U-9Mo and some of the FCM fuel cases. However, it would be expected for the maximum temperatures in the FCM fuel cases to go up by 200–300 degrees when irradiated due to degradation of the thermal conductivity of SiC. However, in all cases, the maximum temperature would be expected to be well below that of UO_2. While the reduction in centerline temperature may provide some benefit for certain design basis accidents, such reductions would not provide significant improvement in coping times under severe accident transients since fuel

Table 8: Required enrichment for ATF.

Fuel[1]	Enrichment (wt% ^{235}U) for target exit burnup[2,3]		
	200 MWh/kgU	600 MWh/kgU	4044 MWh/bundle
UO_2	**0.711**%	1.30%	**0.711**%
UO_2 + 3% SiC (zirc4 clad)	**0.72**%	1.32%	*0.72*%
UO_2 + 3% SiC (SiC clad)	**0.711**%	*1.30*%	*0.72*%
UO_2 + 3% SiC (zirc4 + FeCrAl clad)	**0.79**%	*1.42*%	*0.80*%
UO_2 + 6% SiC	0.72%		
UO_2 + 10% SiC	**0.73**%	*1.34*%	*0.76*%
UN	<**0.711**%; NU = 231.8 MWh/kgU	1.22%	
UN + 3% U_3Si_2	<0.711%; NU = 231.2 MWh/kgU		
UN + 6% U_3Si_2	<0.711%; NU = 230.6 MWh/kgU		
UN + 10% U_3Si_2	<**0.711**%; NU = 229.7 MWh/kgU		
UN + 10% ZrN	<0.711%; NU = 210.4 MWh/kgU		
U-9Mo	**0.93**%	*1.58*%	*0.87*%
UO_2 FCM 35% packing	1.07%		1.89%
UO_2 FCM 40% packing[4]	1.01%	1.80%	**1.62**%
UO_2 FCM 45% packing	0.95%		1.43%
UO_2 FCM 50% packing	0.91%		1.28%
UO_2 FCM 55% packing	0.88%	*1.60*%	1.16%
UN FCM 35% packing	0.93%		1.28%
UN FCM 40% packing	0.89%		**1.13**%
UN FCM 45% packing	0.85%		1.02%
UN FCM 50% packing	0.82%		0.93%
UN FCM 55% packing	0.80%		0.87%
UN TRISO 55% packing	1.12%		**2.25**%

[1]Cladding is zircaloy-4 unless otherwise indicated. [2]*Italicised* values are for cases which were interpolated from supplemental data and not directly analyzed. [3]**Bolded** values are values used for Figure 5. [4]With bare kernel diameters of 650 μm, 700 μm, and 750 μm. Other cases were tested with only 700 μm kernels.

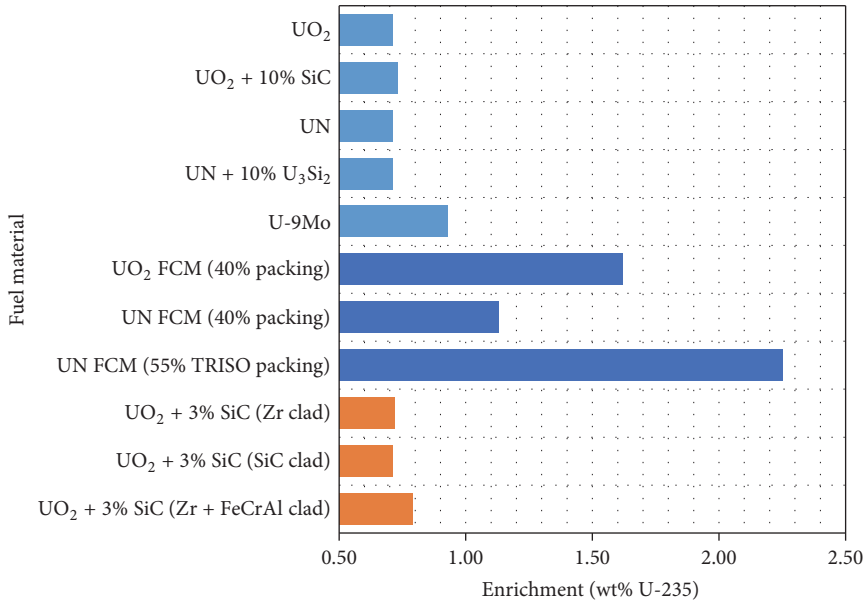

Figure 5: Enrichment requirements for UO_2 and ATF cases.

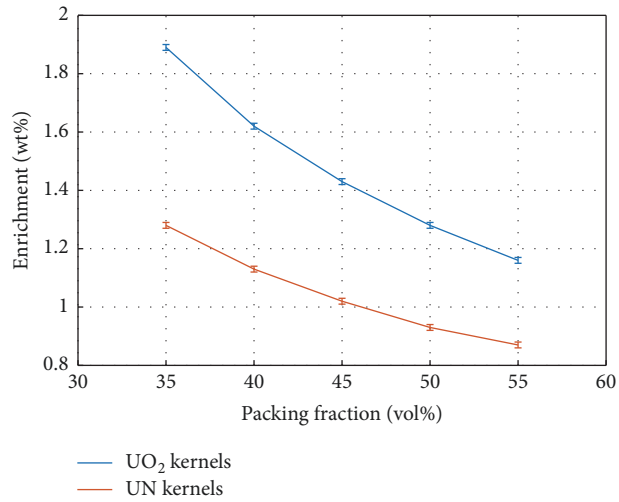

Figure 6: Enrichment requirements for FCM fuel for 4044 MWh/bundle exit burnup.

Table 9: Estimated temperature of fresh and midburnup UO_2-SiC fuel.

Fuel	Fresh fuel temperature (K)	Midburnup temperature[1] (K)
UO_2	2070	2306
UO_2 + 10% SiC	1464	1881
Difference (K)	606	425
Difference (%)	29%	18%

[1]Does not account for changes in fuel-clad gap conductivity or in-pin flux depression.

heat-up would occur relatively quickly after the loss of heat sink.

4.3. Determination of Reactor Physics Parameters. Overall, there are moderate differences between the different cases in terms of coolant void reactivity and fuel temperature coefficient, as seen in Figure 8. In general, for the cases studied, the greater the uranium density, the greater the coolant void reactivity. The dense fuels have a greater CVR than UO_2, while fuels containing significant amounts of SiC have a smaller CVR. More detailed information is given in Table 11.

4.4. Accident Transient Analysis. The results of the stylized transient were found to be similar irrespective of ATF design. As a result of the positive coolant void reactivity for CANDU, power increases fairly rapidly until the transient is turned over by negative reactivity inserted by the reactor's shutdown systems [34]. The rate at which power increases, shown in Figure 9, is influenced by the coolant void reactivity and by the prompt generation time. For CANDU reactors, the prompt generation time is on the order of 10^{-3} seconds, which is significantly longer than for LWRs, due to the larger fuel spacing and reduced enrichment. When comparing the different fuels, the prompt generation time is shorter for UN and U-9Mo due to the increased enrichment, increased uranium density, and additional absorbing material, while for FCM fuel the reduced uranium density increases the prompt generation time. This is reflected by the transient results. UN and U-9Mo fuel has a larger power spike due to the higher CVR and shorter prompt generation time, while FCM fuel has a smaller power spike due to the lower CVR and longer prompt generation time. However, in all cases, the energy deposition is found not to result in any substantial fuel temperature rise.

The postblowdown heat-up phase is governed primarily by the heat capacity of the fuel and cladding material, distribution of decay power, and thermal radiation between the fuel rings and pressure tube. Initially, the outer ring is at the highest temperature due to a higher decay power, particularly for more strongly absorbing fuel where the spatial self-shielding effect is stronger. However, at higher temperatures, this becomes inverted, with the centre pin being hottest, as the other three rings insulate one another and the centre pin. In all cases, however, the peak temperature is in a narrow range between 1800 K and 2000 K. Therefore, in terms of fuel temperature behaviour, the choice of fuel material does not have a substantial effect on the progression of an accident. However, since U-9Mo has a melting point of only around 1400 K, fuel melting will occur for this fuel material before the pressure tube can sag and the moderator can be established as a heat sink. Therefore, in terms of progression of a LOCA-LOECC accident, or similar degraded-cooling scenarios such as a SBO, ATF options do not provide a substantial advantage over UO_2 in delaying severe consequences, as the progression of these accidents is governed by large nonfuel heat sinks, such as the moderator and shield tank water. The U-9Mo case in particular is inferior due to the fuel melting which occurs much sooner than for UO_2.

Two of the cases tested are shown in Figure 10.

5. Discussion

The most modest change from standard UO_2 fuel in zircaloy cladding is to create a UO_2-SiC composite fuel. Overall, the addition of SiC adds negligible parasitic absorption, but the displacement of UO_2 must be compensated by a very slight enrichment in order to achieve the same exit burnup, and slightly more to achieve the same bundle energy. However, the temperature reduction is significant for just 10% of the fuel volume being SiC, as the centre-line temperature is reduced by about 30% for fresh fuel, or about 20% for irradiated fuel. In terms of physics parameters, there is a small but significant reduction in CVR, with only a slight effect on FTC.

Uranium nitride has the potential downside of natural nitrogen being a strong neutron absorber, requiring significant uranium enrichment to compensate and reducing the uranium economy of the fuel cycle. To avoid this, nitrogen enriched in ^{15}N can be used, as ^{15}N is relatively transparent to neutrons. When this is done, the exit burnup is greater than that of UO_2 fuel, which, along with a higher uranium density, allows refueling rates to be reduced significantly. The fuel also has a more negative FTC at midburnup, which is favourable. However, the CVR is somewhat greater for UN fuel than it is for UO_2 fuel.

Table 10: Fuel temperatures calculated for ATF cases.

Fuel	Enrich.	Outer ring temperature (K) Power = 880 kW			Average pin temperature (K) Power = 700 kW		
		Fuel CL	Fuel Avg.	Clad	Fuel CL	Fuel Avg.	Clad
UO_2	0.711%	2069.6	1248.4	608.3	1437.0	981.6	593.9
	1.30%	2159.0	1290.1	610.5	1429.1	979.4	593.9
UO_2 + 3% SiC (zirc4 clad)	0.72%	1760.3	1124.4	608.2	1269.7	913.5	593.9
	1.32%	1835.4	1157.7	610.4	1264.0	911.8	593.9
UO_2 + 3% SiC (SiC clad)	0.711%	1704.9	1087.0	596.6	1239.4	890.8	585.7
UO_2 + 3% SiC (FeCrAl clad)	0.79%	1779.2	1132.1	611.9 (zirc4) 593.9 (FeCrAl)	1269.0	913.0	596.2 (zirc4) 583.7 (FeCrAl)
UO_2 + 6% SiC	0.72%	1607.6	1064.4	608.0	1190.9	880.6	593.9
UO_2 + 10% SiC	0.73%	1463.7	1007.1	607.9	1115.5	848.5	593.9
UN	0.711%	868.5	760.8	610.1	772.1	697.2	593.9
	1.22%	881.4	769.9	612.6	770.9	696.8	593.9
UN + 3% U_3Si_2	0.711%	870.9	762.1	610.1	773.8	698.1	593.9
UN + 6% U_3Si_2	0.711%	873.0	763.2	610.0	775.7	699.1	593.9
UN + 10% U_3Si_2	0.711%	876.2	764.9	610.0	778.3	700.5	593.9
UN + 10% ZrN	0.711%	856.9	753.8	609.3	767.0	694.4	593.9
U-9Mo	0.93%	825.1	742.3	612.1	740.6	682.3	593.9
UO_2 FCM 35% packing	1.07%	814.8	727.0	605.9	744.2	681.5	593.9
	1.89%	821.5	731.5	607.1	743.9	681.4	593.9
UO_2 FCM 40% packing	1.01%	836.0	737.3	606.1	758.5	688.4	593.9
	1.62%	842.3	741.4	607.1	758.1	688.3	593.9
	1.80%	843.7	742.4	607.3	758.0	688.2	593.9
UO_2 FCM 45% packing	0.95%	862.1	749.8	606.2	775.8	696.6	593.9
	1.43%	867.9	753.5	607.1	775.4	696.5	593.9
UO_2 FCM 50% packing	0.91%	893.7	765.0	606.4	796.7	706.6	593.9
	1.28%	899.2	768.4	607.2	796.3	706.5	593.9
UO_2 FCM 55% packing	0.88%	933.4	784.0	606.6	822.7	719.1	593.9
	1.16%	938.7	787.3	607.3	822.3	719.0	593.9
UN FCM 35% packing	0.93%	772.7	707.6	606.7	712.9	666.4	593.9
	1.28%	775.9	709.8	607.4	712.8	666.3	593.9
UN FCM 40% packing	0.89%	779.6	711.1	607.0	717.0	668.4	593.9
	1.13%	782.1	712.9	607.5	716.9	668.3	593.9
UN FCM 45% packing	0.85%	786.4	714.7	607.2	721.2	670.4	593.9
	1.02%	788.3	716.1	607.7	721.1	670.3	593.9
UN FCM 50% packing	0.82%	793.1	718.3	607.5	725.3	672.4	593.9
	0.93%	794.5	719.3	607.8	725.2	672.4	593.9
UN FCM 55% packing	0.80%	799.3	721.8	607.7	729.1	674.4	593.9
	0.97%	800.5	722.6	608.0	729.0	674.4	593.9
UN TRISO 55% packing	2.25%	988.0	813.7	607.1	861.6	739.5	593.9

Table 11: Coolant void reactivity and fuel temperature coefficient for ATF.

Description	Enrichment (wt% ^{235}U)	Fresh fuel k_∞	Fresh fuel		Midburnup	
			CVR (mk)	FTC (pcm/K)	CVR (mk)	FTC (pcm/K)
UO_2	0.711%	1.11850	16.79 ± 0.07	−1.22 ± 0.03	14.59 ± 0.09	−0.12 ± 0.03
	1.300%	1.35036	12.13 ± 0.06	−0.83 ± 0.02	16.24 ± 0.10	−0.16 ± 0.04
UO_2 + 3% SiC	0.720%	1.12319	16.49 ± 0.07	−1.24 ± 0.03	14.37 ± 0.09	−0.18 ± 0.03
	1.320%	1.35597	11.97 ± 0.06	−0.88 ± 0.02	15.82 ± 0.09	−0.17 ± 0.04
UO_2 + 6% SiC	0.720%	1.12203	16.27 ± 0.07	−1.27 ± 0.03	13.98 ± 0.09	−0.19 ± 0.03
UO_2 + 10% SiC	0.730%	1.12577	16.05 ± 0.07	−1.33 ± 0.03	13.70 ± 0.09	−0.16 ± 0.03
UN	0.711%	1.11918	18.14 ± 0.08	−1.30 ± 0.03	17.16 ± 0.10	−0.56 ± 0.04
	1.220%	1.32137	13.78 ± 0.06	−0.98 ± 0.02	19.53 ± 0.10	−0.59 ± 0.04
UN + 3% U_3Si_2	0.711%	1.11907	18.16 ± 0.08	−1.28 ± 0.03	17.33 ± 0.10	−0.59 ± 0.04
UN + 6% U_3Si_2	0.711%	1.11929	18.11 ± 0.08	−1.28 ± 0.03	17.35 ± 0.10	−0.52 ± 0.04
UN + 10% U_3Si_2	0.711%	1.11905	18.26 ± 0.08	−1.27 ± 0.03	17.29 ± 0.10	−0.61 ± 0.04
UN + 10% ZrN	0.711%	1.11744	17.63 ± 0.08	−1.32 ± 0.03	16.00 ± 0.09	−0.51 ± 0.03
U-9Mo	0.930%	1.12952	19.15 ± 0.08	−1.01 ± 0.03	20.02 ± 0.10	−1.05 ± 0.04
UO_2 FCM in SiC 35% packing fraction	1.070%	1.18147	12.05 ± 0.06	−1.75 ± 0.02	10.39 ± 0.07	−0.48 ± 0.03
	1.890%	1.41177	8.68 ± 0.05	−1.15 ± 0.02	9.79 ± 0.07	−0.30 ± 0.03
UO_2 FCM in SiC 40% packing fraction	1.010%	1.17808	12.34 ± 0.06	−1.66 ± 0.02	10.30 ± 0.07	−0.38 ± 0.03
	1.620%	1.37165	9.40 ± 0.05	−1.18 ± 0.02	9.94 ± 0.07	−0.09 ± 0.03
	1.800%	1.41008	8.93 ± 0.05	−1.11 ± 0.02	9.97 ± 0.07	−0.26 ± 0.03
UO_2 FCM in SiC 45% packing fraction	0.950%	1.16881	12.89 ± 0.06	−1.65 ± 0.02	10.62 ± 0.07	−0.25 ± 0.03
	1.430%	1.33787	10.11 ± 0.05	−1.24 ± 0.02	10.17 ± 0.08	0.01 ± 0.03
UO_2 FCM in SiC 50% packing fraction	0.910%	1.16434	13.14 ± 0.06	−1.57 ± 0.02	10.81 ± 0.07	−0.20 ± 0.03
	1.280%	1.30639	10.69 ± 0.06	−1.28 ± 0.02	10.62 ± 0.08	0.05 ± 0.03
UO_2 FCM in SiC 55% packing fraction	0.880%	1.16149	13.39 ± 0.06	−1.53 ± 0.02	10.94 ± 0.08	−0.17 ± 0.03
	1.160%	1.27726	11.28 ± 0.06	−1.28 ± 0.02	10.81 ± 0.08	0.06 ± 0.03
UO_2 FCM (650 μm) in SiC 40% packing fraction	1.010%	1.17804	12.43 ± 0.06	−1.70 ± 0.02	10.50 ± 0.07	−0.37 ± 0.03
	1.620%	1.37161	9.32 ± 0.05	−1.21 ± 0.02	9.95 ± 0.08	−0.12 ± 0.03
UO_2 FCM (750 μm) in SiC 40% packing fraction	1.010%	1.17809	12.54 ± 0.06	−1.69 ± 0.02	10.38 ± 0.07	−0.39 ± 0.03
	1.620%	1.37170	9.34 ± 0.05	−1.20 ± 0.02	9.84 ± 0.08	−0.10 ± 0.03
UN FCM in SiC 35% packing fraction	0.930%	1.16290	12.96 ± 0.07	−1.66 ± 0.02	10.67 ± 0.07	−0.29 ± 0.03
	1.280%	1.29615	10.66 ± 0.06	−1.33 ± 0.02	10.49 ± 0.08	−0.14 ± 0.03
UN FCM in SiC 40% packing fraction	0.890%	1.15883	13.38 ± 0.06	−1.64 ± 0.02	11.10 ± 0.08	−0.26 ± 0.03
	1.130%	1.25901	11.61 ± 0.06	−1.36 ± 0.02	11.19 ± 0.08	−0.18 ± 0.03
UN FCM in SiC 45% packing fraction	0.850%	1.15066	13.93 ± 0.07	−1.61 ± 0.02	11.52 ± 0.08	−0.22 ± 0.03
	1.020%	1.22738	12.48 ± 0.06	−1.40 ± 0.02	11.45 ± 0.09	0.03 ± 0.03
UN FCM in SiC 50% packing fraction	0.820%	1.14447	14.37 ± 0.07	−1.55 ± 0.03	11.90 ± 0.08	−0.23 ± 0.03
	0.930%	1.19745	13.32 ± 0.06	−1.43 ± 0.02	11.97 ± 0.08	−0.09 ± 0.03
UN FCM in SiC 55% packing fraction	0.800%	1.14123	14.79 ± 0.07	−1.54 ± 0.03	12.61 ± 0.08	−0.26 ± 0.03
	0.970%	1.17653	14.03 ± 0.07	−1.44 ± 0.03	12.59 ± 0.09	−0.19 ± 0.03
UN FCM in SiC 55% TRISO packing fraction	2.250%	1.46143	7.86 ± 0.05	−1.14 ± 0.02	9.46 ± 0.07	−0.04 ± 0.03
UO_2 + 3% SiC zircaloy cladding	0.720%	1.12319	16.49 ± 0.07	−1.24 ± 0.03	14.37 ± 0.09	−0.18 ± 0.03
UO_2 + 3% SiC SiC cladding	0.711%	1.12010	16.10 ± 0.08	−1.27 ± 0.03	13.84 ± 0.09	−0.22 ± 0.03
UO_2 + 3% SiC zircaloy + FeCrAl cladding	0.790%	1.12855	16.03 ± 0.08	−1.20 ± 0.03	14.33 ± 0.09	−0.21 ± 0.03

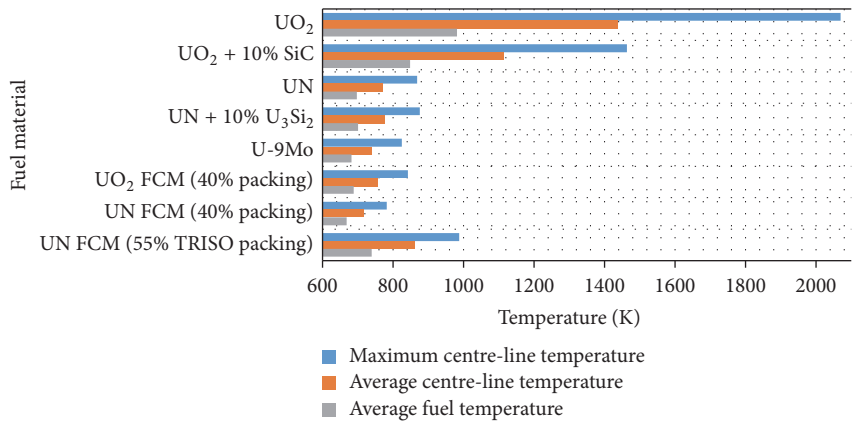

Figure 7: Fuel temperatures for UO_2 and ATF cases.

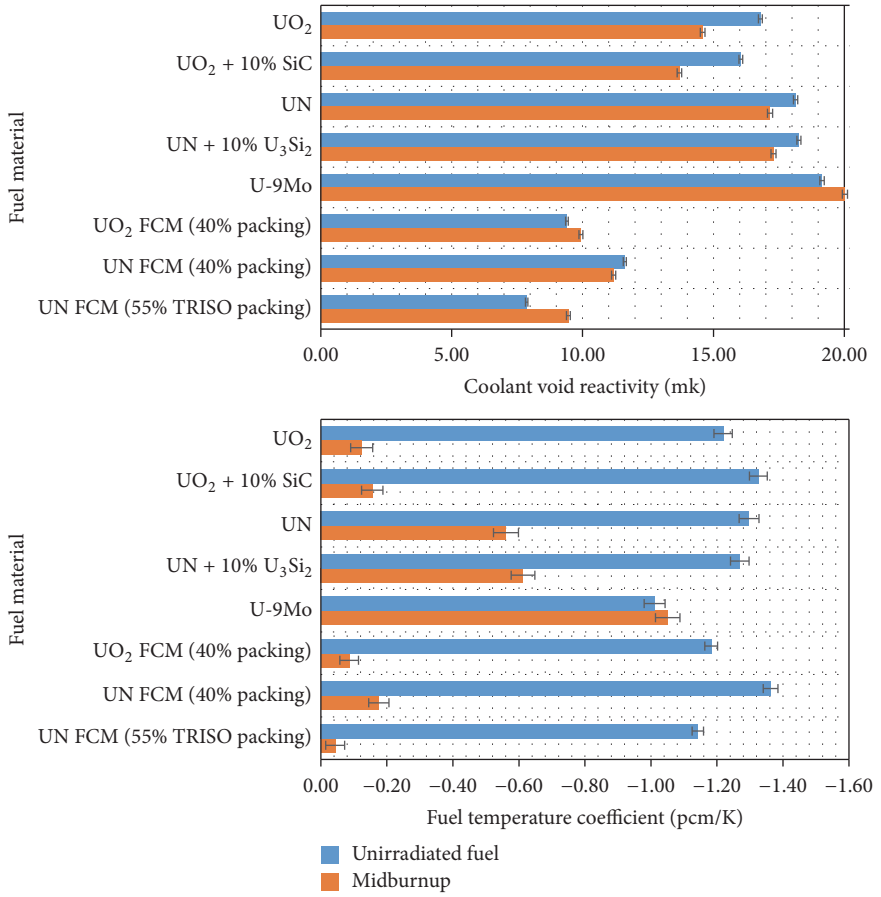

Figure 8: CVR and FTC for UO_2 and ATF cases.

Adding U_3Si_2 to UN reduces the exit burnup only slightly. Adding ZrN to make a (U, Zr)N solution reduces the exit burnup significantly, although, even with 10% ZrN by volume, the exit burnup is still better than for UO_2. Adding ZrN can improve compatibility with CANDU to some extent as it changes the exit burnup, bundle weight, and CVR to be closer to the values of the standard UO_2 bundles, while retaining a low fuel temperature and more favourable FTC.

Uranium-molybdenum fuel also requires enrichment (0.93% for the same exit burnup) as molybdenum also contributes to parasitic absorption, though not as severely as nitrogen. However, as the uranium density is significantly greater than it is for UO_2, the fuel lasts longer in the core for this same exit burnup. Also, the fuel temperature coefficient remains significantly negative even with irradiation. However, U-9Mo fuel has several disadvantages. A greater

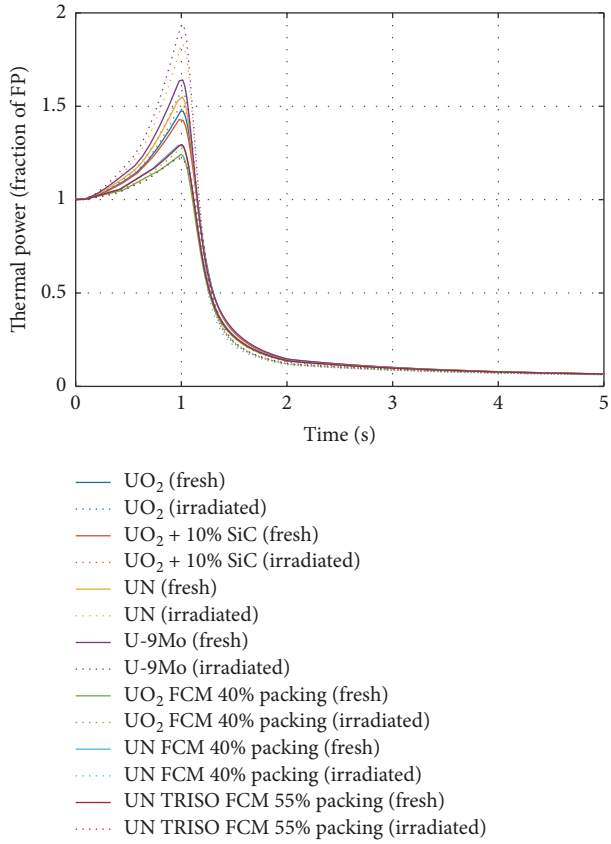

Figure 9: Reactor power transient for UO_2 and ATF.

coolant void reactivity results in a larger power pulse in a LOCA event. More importantly, though, the melting point is low enough that the fuel can melt in a number of accident scenarios for which UO_2 fuel or other ATF candidates would easily survive.

Fully ceramic microencapsulated fuel, in terms of uranium density, is the opposite of UN and U-9Mo fuel, as the uranium density is lower for bare UO_2 or UN kernels in a SiC matrix compared to solid UO_2 and is even lower for true FCM fuel where TRISO particles are embedded in a SiC matrix. Therefore, even though the SiC matrix contributes to very little parasitic absorption, significant enrichment is required to achieve the same energy per bundle as a UO_2 bundle. The CVR is significantly less for FCM fuel compared to UO_2 fuel, with a lower uranium density corresponding to a lower CVR. However, the FTC for FCM fuel is generally slightly less negative at midburnup compared to the corresponding solid fuel and is even slightly positive for some cases with UO_2 kernels. The effect on FCM is a combination of a positive contribution from the material change and a negative contribution from the reduced fuel temperature.

Changing the cladding also has a small effect on reactor physics. Silicon carbide has a beneficial effect as it is more transparent to neutrons than zircaloy; thus the fuel enrichment can be reduced by about 0.01%. On the other hand, FeCrAl coating requires roughly a 0.07% increase in enrichment for the case it was tested on, despite the fact that only 20% of the cladding thickness was replaced. Small but significant reductions in CVR were noted, while changes in FTC were insignificant.

Given the above, in the transient scenario modelled no substantial advantage can be identified for any of the ATF candidates over UO_2. The progression of a severe accident in a CANDU reactor is largely governed by several large heat sinks, including the moderator and shield tank water. These heat sinks, along with structural materials such as pressure tubes, are independent of any changes to the fuel materials, and they have a large heat capacity compared to the fuel itself. Since decay heat is governed by the reactor's operating power history and energy deposition in a transient and not by the fuel composition, the accident is expected to progress at a similar rate regardless of the fuel composition. The primary exception is for U-9Mo fuel, which is actually inferior to UO_2 fuel due to premature melting in a number of scenarios.

Despite this, there are a few places where, qualitatively, ATF can be expected to have an advantage over UO_2. The first advantage is in terms of fission product retention within fuel pellets. Lowering the fuel temperature is expected to reduce the diffusion rate of certain fission products into the fuel-clad gap. In the case of fuel damage where the cladding fails, only these fission products escape, while those trapped within the fuel pellets are retained. In addition, FCM-type fuels provide additional barriers to fission product release. However, in all cases, including for UO_2, the radiation release due to cladding failure is not expected to be substantial.

The second advantage applies to ATF cladding, for which a reduction in hydrogen generation is expected under certain accident conditions compared to zircaloy, reducing the risk of further failures leading to a hydrogen explosion. SiC cladding can potentially withstand high temperatures without significant oxidation. By contrast, however, FeCrAl has a lower melting point than zircaloy and would actually melt under the stylized accident scenario that was modelled, though zircaloy oxidation would still be delayed compared to not having the coating.

The primary disadvantage for ATF over the current standard UO_2 fuel is the need for enrichment. Even for a UO_2-SiC composite bundle with 10% SiC, while it can be used without enrichment, the energy that can be extracted from one fuel bundle is reduced by about 25%, which has economic implications. U-9Mo and FCM result in a subcritical or barely critical core. Applying a FeCrAl surface layer to the cladding also substantially reduces exit burnup unless the fuel is enriched. Even the very slight enrichment predicted for UO_2-SiC composite bundles would require the establishment of new infrastructure, substantially raising costs even if relatively little enrichment is required. This is in contrast to ATF considerations for LWRs, where an increase in enrichment from, for example, 4.8% to 5.0%, would not require significant infrastructure changes. Economically, considering ATF for CANDU reactors is more reasonable in the case where the fuel input is not natural uranium, such as if a CANDU is being fueled by recycled uranium (from used LWR fuel), MOX, thorium, or any combination of those with each other or with natural or depleted uranium. In this case, the slight enrichments required for ATF can be

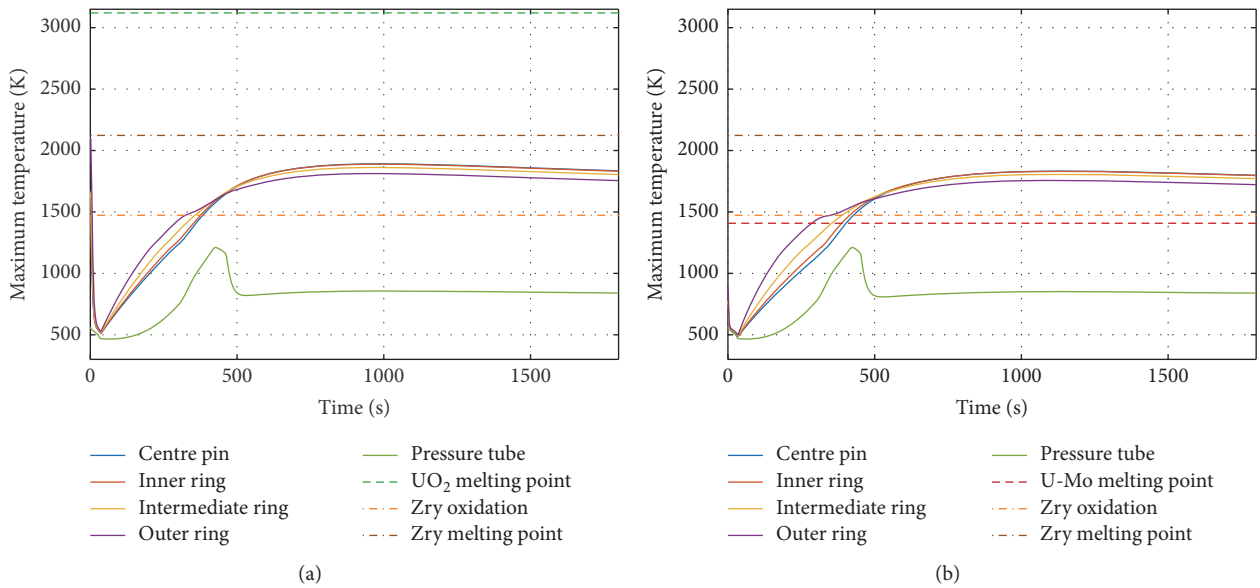

Figure 10: Fuel temperature behaviour for selected cases: UO_2 (a) and U-9Mo (b).

accommodated more easily. However, the reactor physics and heat transfer properties would have to be reevaluated for the fuel change.

There are two primary exceptions. The first exception is for the UN-based fuel materials, when enriched in ^{15}N. These fuels have a significant neutron economy advantage over UO_2, which permits an improved exit burnup even with natural uranium. The second exception is for SiC cladding, which has a better neutron economy than zircaloy. However, since this study did not consider the mechanical properties of the selected materials, this result assumes that the bundle and pin geometries do not change. If it is found that the SiC cladding must be made thicker to permit manufacturing or to compensate for its mechanical properties, then the neutron economy advantage will be lost due to a reduction in fuel volume.

More generally, changes to the fuel geometry were not considered in this study. One possibility that could affect the fuel properties would be changing to 43-element CANFLEX fuel or to some other geometry with different pin sizes. ATF materials improve the safety margin over UO_2 for centreline temperature, potentially permitting the use of bundles with fewer, larger pins to increase the fuel volume. However, such a change would reduce the fuel surface area and thus reduce the margin to critical heat flux (CHF) and so cannot be done if CHF is the limiting factor. Alternatively, if centreline temperature is the limiting factor, the maximum bundle power and possibly the reactor power can be uprated. Since CHF for high-density fuel is a potential issue, that fuel could potentially benefit from geometry with smaller pins for the outer ring, such as the CANFLEX bundle or possibly a fuel-specific bundle with even greater differences in pin diameters. Another possibility would be to use graded enrichments, with the fuel in the outer ring having a lesser enrichment than the rest of the fuel.

6. Conclusions

The primary findings of this study are as follows:

(i) UO_2 with SiC cladding, along with UN fuel enriched in ^{15}N, permits the use of natural uranium. All other ATF concepts that were evaluated lead to requiring enrichment of uranium. If the uranium is not enriched, either a significant burnup penalty is taken or the core is subcritical. Since most current CANDUs run on natural uranium, particularly in Canada, ATF concepts requiring enrichment would require the establishment of enrichment infrastructure or import of slightly enriched uranium from other countries. If UN fuel is adopted, nitrogen enrichment facilities would be required instead.

(ii) In a number of severe accident scenarios that were considered, changing the fuel to ATF would not extend the time between the onset of the accident and the onset of fuel melting. The propagation of the accident generally allows the moderator, and possibly the shield tank water, to act as a heat sink for the fuel's decay heat to prevent melting. The size of these heat sinks and the amount of decay heat are independent of the fuel material, and as these heat sinks are large relative to the heat capacity of the fuel, changing the fuel has relatively little effect on when melting will occur. The key exception is U-9Mo, which has a melting point of roughly 1400 K and so heat transfer to the moderator is not sufficient to prevent melting, making this material accident-*intolerant* relative to UO_2 under this scenario.

(iii) All ATF fuel pellet materials reduce the fuel temperature compared to UO_2 and can potentially reduce the diffusion rate of fission products into the fuel-clad gap. This can reduce the magnitude of radiation

release in the case of cladding failure. However, this effect was not quantified in this study, and the significance of this advantage depends on whether the predicted releases from UO_2 fuel under cladding failure (no fuel melting) can be accepted.

(iv) In an accident scenario, it is predicted that cladding temperatures are hot enough to result in extensive oxidation. Therefore, oxidation-resistant cladding can delay or prevent the oxidation of cladding and production of hydrogen gas. Again, evaluation of this effect was beyond the scope of the models used in this study, but the results of this study show that it would be useful for future studies to evaluate the extent of cladding oxidation and hydrogen generation, and the comparative risk of a hydrogen explosion for each case.

Further studies are needed to evaluate the full-core behaviour of the fuel, possible changes to fuel geometry, and the mechanical behaviour of the fuel and cladding materials in normal and accident conditions. In addition, a more detailed economic analysis should be carried out to determine whether it is viable to switch to accident-tolerant fuel, weighing increased costs due to enrichment and fuel manufacturing against the reduced level of risk and also weighing the costs against the costs of other modifications that can be made to the station to reduce the risk of severe accident consequences.

While some cases, such as U-9Mo, can be immediately ruled out from consideration, additional cases not analyzed in this study could be considered. This can include fuel with other "dopant" materials mixed in to improve thermal conductivity. It can also go beyond simple material changes, such as changing the bundle geometry (e.g., to CANFLEX) or using different compositions for different rings, which can improve bundle power distribution but increase the complexity of the bundle for manufacture.

In most cases, an economic disadvantage is probable as either uranium enrichment is needed or the fuel otherwise becomes more expensive to manufacture (which can be expected for silicon carbide cladding). Uranium nitride enriched in ^{15}N may provide an economic advantage by increasing the exit burnup and reducing fueling machine loading, but economic savings would depend on the cost of nitrogen enrichment and fuel manufacture. A cost analysis would be required to determine whether the benefits of an increased exit burnup would exceed the increase in fuel cost per bundle.

Conflicts of Interest

The authors declare no conflicts of interest regarding the publication of this paper.

References

[1] International Atomic Energy Agency, *Thermophysical Properties Database of Materials for Light Water Reactors and Heavy Water Reactors*, International Atomic Energy Agency, Vienna, Austria.

[2] L. Haacke, *Principles of Nuclear Safety, Course 4.3, Module 03 - Defence in Depth*, CANTEACH, 1996.

[3] J. C. Luxat, "Thermal-hydraulic aspects of progression to severe accidents in CANDU reactors," *Nuclear Technology*, vol. 167, no. 1, pp. 187–210, 2009.

[4] A. Labib and M. J. Harris, "Learning how to learn from failures: The Fukushima nuclear disaster," *Engineering Failure Analysis*, vol. 47, pp. 117–128, 2015.

[5] E. J. Lahoda, L. Hallstadius, F. Boylan, and S. Ray, "What should be the objective of accident tolerant fuel?" in *Proceedings of the 2014 Annual Meeting on Transactions of the American Nuclear Society and Embedded Topical Meeting: Nuclear Fuels and Structural Materials for the Next Generation Nuclear Reactors, NSFM 2014*, pp. 733–736, usa, June 2014.

[6] D. Permar, A. Cartas, and H. Wang, "Innovative accident tolerant UO2 composite fuel for use in LWRs," in *Proceedings of the 2013 Winter Meeting on Transactions and Embedded Topical Meetings: Risk Management for Complex Socio-Technical Systems, 2nd ANS SMR 2013 Conference, Nuclear Nonproliferation - 1st Fission to the Future*, pp. 185-186, usa, November 2013.

[7] D. Permar, Z. Chen, and J. Tulenko, "Enhanced accident tolerant UO2-diamond composite fuel pellets prepared by SPS," in *Proceedings of the 2013 Winter Meeting on Transactions and Embedded Topical Meetings: Risk Management for Complex Socio-Technical Systems, 2nd ANS SMR 2013 Conference, Nuclear Nonproliferation - 1st Fission to the Future*, pp. 267–269, usa, November 2013.

[8] K. Y. Spencer, L. Sudderth, R. A. Brito et al., "Sensitivity study for accident tolerant fuels: Property comparisons and behavior simulations in a simplified PWR to enable ATF development and design," *Nuclear Engineering and Design*, vol. 309, pp. 197–212, 2016.

[9] P. Malkki, "The manufacturing of uranium nitride for possible use in light water reactors," 2015.

[10] J. J. Powers, W. J. Lee, F. Venneri et al., "Fully Ceramic Microencapsulated (FCM) Replacement Fuel for LWRs," Tech. Rep. ORNL/TM-2013/173, 2013.

[11] L. H. Ortega, J. Evans, and S. M. McDeavitt, "Development of a high density uranium nitride-uranium silicide composite accident tolerant fuel," in *Proceedings of the 2014 Annual Meeting on Transactions of the American Nuclear Society and Embedded Topical Meeting: Nuclear Fuels and Structural Materials for the Next Generation Nuclear Reactors, NSFM 2014*, pp. 999-1000, usa, June 2014.

[12] J. M. Harp, P. A. Lessing, and R. E. Hoggan, "Uranium silicide fabrication for use in LWR accident tolerant fuel," in *Proceedings of the 2014 Annual Meeting on Transactions of the American Nuclear Society and Embedded Topical Meeting: Nuclear Fuels and Structural Materials for the Next Generation Nuclear Reactors, NSFM 2014*, pp. 990–993, usa, June 2014.

[13] J. Creasy, "Thermal Properties of Uranium-Molybdenum Alloys: Phase Decomposition Effects of Heat Treatments," 2011.

[14] R. A. Brown, C. Blahnik, and A. P. Muzumdar, "DEGRADED COOLING IN A CANDU REACTOR.," *Nuclear Science and Engineering*, vol. 88, no. 3, pp. 425–435, 1984.

[15] G. J. Youinou and R. S. Sen, "Impact of accident-tolerant fuels and claddings on the overall fuel cycle: A preliminary systems analysis," *Nuclear Technology*, vol. 188, no. 2, pp. 123–138, 2014.

[16] D. Burkes, G. Mickum, and D. Wachs, *Thermophysical Properties of U-10Mo Alloy*, 2010.

[17] J.-H. Chun, S.-W. Lim, B.-D. Chung, and W.-J. Lee, "Safety evaluation of accident-tolerant FCM fueled core with SiC-coated zircalloy cladding for design-basis-accidents and beyond DBAs," *Nuclear Engineering and Design*, vol. 289, pp. 287–295, 2015.

[18] L. J. Ott, K. R. Robb, and D. Wang, "Preliminary assessment of accident-tolerant fuels on LWR performance during normal operation and under DB and BDB accident conditions," *Journal of Nuclear Materials*, vol. 448, no. 1–3, pp. 520–533, 2014.

[19] B. Cheng, Y.-J. Kim, and P. Chou, "Improving Accident Tolerance of Nuclear Fuel with Coated Mo-alloy Cladding," *Nuclear Engineering and Technology*, vol. 48, no. 1, pp. 16–25, 2016.

[20] X. Wu, T. Kozlowski, and J. D. Hales, "Neutronics and fuel performance evaluation of accident tolerant FeCrAl cladding under normal operation conditions," *Annals of Nuclear Energy*, vol. 85, pp. 763–775, 2015.

[21] C. P. Deck, G. M. Jacobsen, J. Sheeder et al., "Characterization of SiC-SiC composites for accident tolerant fuel cladding," *Journal of Nuclear Materials*, vol. 466, pp. 1–15, 2015.

[22] X. Wu, P. Sabharwall, and J. Hales, "Neutronics and Fuel Performance Evaluation of Accident Tolerant Fuel under Normal Operation Conditions," Tech. Rep. INL/EXT-14-32591, 2014.

[23] N. M. George, K. Terrani, J. Powers, A. Worrall, and I. Maldonado, "Neutronic analysis of candidate accident-tolerant cladding concepts in pressurized water reactors," *Annals of Nuclear Energy*, vol. 75, pp. 703–712, 2015.

[24] J. M. Harp, P. A. Lessing, and R. E. Hoggan, "Uranium silicide pellet fabrication by powder metallurgy for accident tolerant fuel evaluation and irradiation," *Journal of Nuclear Materials*, vol. 466, pp. 1–11, 2015.

[25] K. D. Johnson, A. M. Raftery, D. A. Lopes, and J. Wallenius, "Fabrication and microstructural analysis of UN-U3Si2 composites for accident tolerant fuel applications," *Journal of Nuclear Materials*, vol. 477, pp. 18–23, 2016.

[26] J. Leppänen, "PSG2/Serpent a Continuous-energy Monte Carlo Reactor Physics Burnup Calculation Code," Tech. Rep., VTT Technical Research Centre of Finland, 2009.

[27] PDE Solutions Inc, *FlexPDE 6 Version 6.40*, PDE Solutions Inc., 2016.

[28] T. L. Rucker and C. M. Johnson, "Relationship between isotopic uranium activities and total uranium at various uranium enrichments," *Journal of Radioanalytical and Nuclear Chemistry*, vol. 235, no. 1-2, pp. 47–52, 1997.

[29] B. Becker, R. Dagan, and G. Lohnert, "Proof and implementation of the stochastic formula for ideal gas, energy dependent scattering kernel," *Annals of Nuclear Energy*, vol. 36, no. 4, pp. 470–474, 2009.

[30] S. C. Cheng and R. I. Vachon, "The prediction of the thermal conductivity of two and three phase solid heterogeneous mixtures," *International Journal of Heat and Mass Transfer*, vol. 12, no. 3, pp. 249–264, 1969.

[31] F. J. Doria, *CANDU Safety #16: Large Loss-of-Coolant Accident with Coincident Loss of Emergency Core Cooling*, Atomic Energy of Canada Limited, 2001.

[32] "Wolfram—Alpha curated data," 2016.

[33] E. W. Lemmon, M. L. Huber, and M. O. McLinden, *NIST Standard Reference Database 23: Reference Fluid Thermodynamic and Transport Properties-REFPROP, Version 9.1*, Gaithersburg, Maryland, 2013.

[34] R. S. Hart and R. A. Olmstead, *CANDU Passive Shutdown Systems*, AECL CANDU, Mississauga, Ontario, Canada.